

Young Blue Straggler Stars in the Galactic Field

Gemunu Ekanayake,^{1*} and Ronald Wilhelm²

¹*Department of Physics, Manhattanville college, Purchase, NY 10577, USA*

²*Department of Physics and Astronomy, University of Kentucky, Lexington, KY 40506, USA*

Accepted XXX. Received YYY; in original form ZZZ

ABSTRACT

In this study we present an analysis of a sample of field blue straggler (BS) stars that show high ultra violet emission in their spectral energy distributions (SED): indication of a hot white dwarf (WD) companion to BS. Using photometry available in the Sloan Digital Sky Survey (SDSS) and Galaxy Evolution Explorer (GALEX) surveys we identified 80 stars with UV excess. To determine the parameter distributions (mass, temperature and age) of the WD companions, we developed a fitting routine that could fit binary model SEDs to the observed SED. Results from this fit indicate the need for a hot WD companion to provide the excess UV flux. The WD mass distribution peaks at $\sim 0.4 M_{\odot}$, suggesting the primary formation channel of field BSs is case B mass transfer, i.e. when the donor star is in red giant phase of its evolution. Based on stellar evolutionary models, we estimate the lower limit of the binary mass transfer efficiency to be $\beta \sim 0.5$.

Key words: blue straggler, white dwarf, binary stars, SDSS, GALEX

1 INTRODUCTION

Blue Straggler stars were first discovered in a photometric study of globular cluster M3 by Sandage in 1953.(Sandage 1953). They are identified by their position in color magnitude diagram, in which they appear along the extension of the main sequence but bluer and brighter than the main sequence turn-off, giving the appearance of a younger stellar population. The BS sequence is a typical feature of most globular clusters. Since Sandage’s discovery, blue stragglers have been observed in many stellar environments, including open star clusters (Mathieu and Geller 2009), globular clusters (Ferraro et al. 1999), dwarf spheroidal galaxies (Momany et al. 2007) and the Galactic field(Preston and Sneden 2000).

The exact mechanism for the formation of blue stragglers is still not fully understood. Single star evolutionary theory fails to explaining the existence of BS stars since it is not possible for stars to have masses greater than the main-sequence turnoff in a single epoch star formation environment. Under the correct circumstances, however, it is possible for stars to gain significant mass long after the star formation epoch has ended. Two leading theories rely on the basic idea that BSs are formed by adding mass to a main sequence star in a binary or multiple stellar system via some interaction mechanism. (1) Mass transfer between two stars in a binary system: This is the case where the more mas-

sive star in a binary system transfers material, during its post main-sequence phase, to its companion star. Though still not fully understood McCrea (McCrea 1964) provided the first, seminal idea of mass transfer and its consequences during binary evolution. If the mass transfer is stable, this may add sufficient mass to the secondary to convert it into a blue straggler. This appears to be the main formation channel for BS stars, particularly in the low density environment of the Galactic field. Convincing evidence for operation of this process was reported by Gosnell et al. (2014) for 3 stars in the old open cluster NGC 188. (2) Merger between stellar systems: This could happen in various scenarios, such as the merger of a contact binary, a merger during a dynamical encounter and a merger of an inner binary in hierarchical triple system. In such a scenario, it is expected that the merged stars will form a single more massive star.

Generally the mass transfer binaries are classified on the basis of the evolutionary phase of the donor (Kippenhahn and Weigert 1967). **Case A:** Mass transfer occurs during hydrogen core burning phase of the donor. This can happen if the orbital separation of the binary is small (usually an orbital period of a few days). **Case B:** Mass transfer occurs after exhaustion of hydrogen in the core of the donor and the donor enters the red giant phase. In this case orbital period is about 100 days or less, but significantly longer than case A. **Case C:** Mass transfer occurs after exhaustion of core helium (He) burning and the donor enters the AGB phase. Here the orbital period is generally greater than 100 days. It is believed that case A mass trans-

* E-mail: gemunu.ekanayake@mville.edu

fer is more likely to be result in the coalescence of the two stars.(Chen and Han 2009) In that sense it can be treated as one of the merger scenarios. According to the binary evolution simulations (Chen and Han 2009), in order to produce a BS via case B or case C, the mass transfer has to be stable. During stable mass transfer the donor stays within its Roche-lobe. Therefore the stability of the mass transfer depends on donor’s response to the mass loss, on how conservative the process is and on the angular momentum loss processes in this binary. Given stable mass transfer, case B will result in a He white dwarf companion bound to the blue straggler, while in case C the remnant companion is a CO white dwarf.

1.1 Field Blue Straggler Stars

For a given stellar population the dominant formation channel of BSs depends on its environment. The BSs in the Galactic field, where the stellar number density is much lower than globular clusters, are formed primarily from binary mass transfer (Preston and Sneden 2000). High resolution study of Field BSs done by Preston and Sneden (Preston and Sneden 2000) suggested that 60 % their sample were binaries. Moreover they concluded that the great majority of field BSs are probably created by Roche-lobe overflow during red giant branch evolution (case B). Ryan et al. (Ryan et al. 2002) studied lithium deficiency and rotation of the BSs and came to the conclusion that these stars can be regarded as mass transfer binaries. The origin of BSs in the Galactic field is clearly tied to the overall formation of the Galactic halo. Since star formation ended in the halo over 10 giga-years ago, most identified BSs originate through case B/C evolution. The exception, as argued by Preston and Landolt (1999), is a modest fraction of BSs that may actually be young, massive stars that have been accreted from Galactic satellites which contain young stellar populations.

To test the theory with observations, it is vital to identify the clean sample of mass transfer candidates. Because blue stragglers in globular clusters are contaminated by those formed via collisions, field blue stragglers are the best candidates for a clean sample of mass-transfer BSs. As mentioned above the mass-transfer process results in a BS with a white dwarf companion. BSs are much brighter than WDs at optical wavelengths so, such binaries are difficult to observe directly. However, if the WD companions to BS are sufficiently young and hot, they can be detected at ultraviolet wavelengths. Studying a sample of such recent BS/WD systems can set constraints on the mass transfer formation mechanism. In this paper we present a study of field BSs that show UV excess in their SED, in order to characterize their mass transfer history. Sections 2 and 3 describe the methodology for identifying the UV excess stars by use of the SDSS and GALEX photometry. Section 4 summarizes our analysis and techniques used to determine the WD parameters. A brief discussion and our conclusions are provided in section 5.

2 DATA

Over the years many photometric studies have been done to identify field BSs, primarily using color-color plots. For example Yanny et al. (2000) identified 2700 field BSs using SDSS photometry. Sirko et al. (2004) used SDSS photometry in combination with spectroscopy to identify field BSs.

The data used for this study were taken from the Sloan Digital Sky Survey Data Release 12 (SDSS DR12) and Galaxy Evolution Explorer (GALEX) GR5, an ultraviolet survey.

2.1 SDSS Data

SDSS DR12 offers the latest data from SDSS project 3. It provides photometry in 5 bands (u, g, r, i and z) for 400 million objects and low resolution spectroscopy with resolution $R \sim 1800$ and wavelength coverage 3800-9200Å, for about 2 million objects.

Field BSs can be identified in a u-g vs g-r diagram by use of the following color cuts.

$$0.60 < (u - g) < 1.60 \quad (1)$$

$$-0.20 < (g - r) < 0.05 \quad (2)$$

This area in the color-color diagram is populated by A-type stars including high gravity BS and low gravity BHB stars. Therefore, in order to separate the BSs from BHB stars one would need stellar parameters for individual stars. For that purpose we employed the current version of the Sloan Extension for Galactic Understanding and Exploration (SEGUE) Stellar Parameter Pipeline (SSPP) (Lee et al. 2008). We select only the BSs above 7000 K to avoid contamination of other F,G type main sequence stars and/or variable RR lyrae stars.

2.2 GALEX Data

GALEX photometry was performed in two ultraviolet(UV) bands Far-UV(FUV) and Near-UV(NUV). The effective wavelengths are 1516 and 2267 angstroms for FUV and NUV bands respectively.

2.3 Cross-Identification of sources

Most GALEX observations were designed to cover the SDSS footprint at a comparable depth. Constructing spectral energy distributions (SEDs) which range from UV to IR requires combining SDSS sources to GALEX counterparts. The matching was done on line by use of the CDS X-Match Service¹, adopting a match radius of 5". Such a match highly depends on the positional accuracy and resolution of both surveys. Because the GALEX images have lower angular resolution there are cases with multiple GALEX-matches per given SDSS source. These comprise about 10% of our total sample. In such cases we used only the closest distance matches. In vast majority of cases (> 90%) GALEX and

¹ <http://cdsxmlmatch.u-strasbg.fr/xmlmatch>

SDSS sources are matched within 2 arc-seconds. Our final sample includes 2188 stars.

SDSS data were corrected for interstellar extinction using the extinction relations given in [Schlafly and Finkbeiner \(2011\)](#) while FUV and NUV were corrected for extinction using the relations given in [Rey et al. \(2007\)](#).

3 UV-EXCESS STARS

Identification of UV-excess stars based on their position in FUV/optical color-color plot is one useful application of UV photometry. Using GALEX and SDSS colors together have enabled the discovery of white dwarf-main sequence (WDMS) binary systems, i.e., binaries with WD primaries and late-type main-sequence secondaries ([Rebassa-Mansergas et al. 2012](#))

[Smith et al. \(2014\)](#) adopted a similar approach to identify the FGK-type stars with excess UV in their spectral energy distribution. They used combined data from GALEX satellite’s far-UV (FUV) and near-UV (NUV) bandpasses as well as from the ground-based SDSS survey and the Kepler Input Catalog to identify stars that exhibit FUV-excesses relative to their NUV fluxes and spectral types. They considered that these UV excesses originate from various types of hot stars, including white dwarf DA and sdB stars, binaries, and strong chromosphere stars that are young or in active binaries. They calibrate the UV-excess stars using their distribution in $(FUV - NUV) - T_{eff}$ plane (Figure 3 [Smith et al. \(2014\)](#)). We adopted a similar method in selecting BS UV-excess stars.

3.1 Temperature Sanity Check

The method for selecting UV excess BSs depend on the temperatures of the stars. Rather than simply adopting the SSPP T_{eff} values directly, we remeasured the temperatures for our sample stars by fitting of the Hydrogen Balmer lines of each SDSS spectrum to model synthetic spectra. A grid of synthetic spectra, spanning the stellar parameter range of our sample, was generated using Kurucz ATLAS12 atmosphere models² and the spectral synthesis routine, SPECTRUM ([Gray and Corbally 1994](#)). In order to achieve a finer grid resolution we interpolate the Kurucz models using kmOD IDL package.³ kmOD interpolates linearly a Kurucz model for the desired values of effective temperature, surface gravity and metallicity using 8 surrounding models. Our final grid consists of spectra with the temperatures in the range 6500 - 10,000 K in steps of 125 K. Finally the point estimates of mean and error in temperatures were calculated. The mean error obtained for temperatures is 140 K. We compared the temperatures obtained from our method to those obtained from the SSPP in order to check the consistency (Figure 1(a)). Both SSPP and our method predicts consistent values for the majority of the stars. We excluded from our sample any stars which have a T_{eff} difference larger than 250 K. Given the larger uncertainties in our measurements, we have adopted the SSPP T_{eff} values for our final sample.

² Kurucz models are available at <http://kurucz.harvard.edu>

³ <http://www.as.utexas.edu/hebe/>

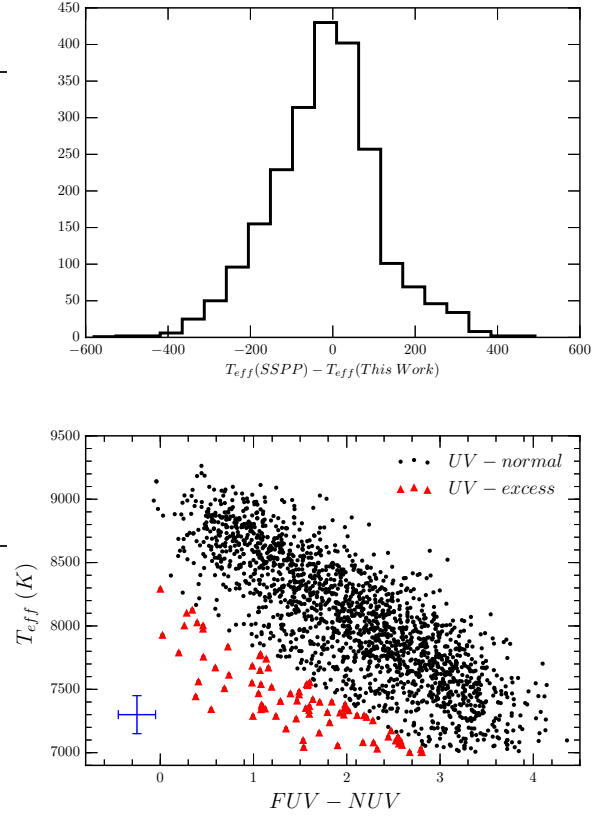


Figure 1. Top: Comparison of temperatures of BSs in this work with SSPP. Bottom: $s(FUV-NUV)$ vs. SSPP temperature values from SDSS-GALEX data. Data represented by red triangles deviate more than 2σ from the fit to the main diagonal sequence and identified as BSs with UV-excess.

We plotted T_{eff} values determined from the SSPP vs $(FUV - NUV)$ color of the stars in our sample (Figure 1). The diagonal sequence in the Figure 1 reflects the relationship between SDSS T_{eff} and $(FUV - NUV)$ for the main-sequence stars. We fit the main diagonal sequence with a quadratic fit and we identify stars lying more than 2 sigma below the regression as UV-excess BS stars. These are our candidates for the BSs with a hot WD companion. Their GALEX and SDSS photometry along with their stellar parameters are given in Table A1.

4 BS-WD SED FITTING

In order to obtain the stellar parameters of BS-WD binaries, we fit the observed SEDs of UV-excess stars with a composite model SEDs composed of BSs and white dwarfs. We employed a theoretical grid of spectra ([Castelli and Kurucz 2004](#)) with $6000 < T_{eff} < 10000$ K in steps of 250 K, $0.5 < \log g < 5.0$ in steps of 0.5, and $-2.5 < [Fe/H] < 0.5$ in steps of 0.5.

For white dwarf models we employed the theoretical color tables developed by Bergeron (University of Montreal; private communication). For these models stellar masses and cooling ages are obtained from a detailed evolutionary cooling sequences appropriate for these stars. For the white

dwarfs with pure hydrogen model atmospheres above temperatures 30,000 K, the carbon-core cooling models of Wood (Wood 1995) with thick hydrogen layers of $M_H/M_* = 10^{-4}$ were used. For temperatures below 30,000 K, cooling models similar to those of Fontaine et al. (2001) but with carbon-oxygen cores and $M_H/M_* = 10^{-4}$ were used.

4.1 Synthetic Fluxes

In the course of fitting procedure we calculate synthetic fluxes for both BS and WD in GALEX and SDSS bandpasses. The synthetic spectra can be converted to a monochromatic flux for a given bandpass via,

$$f = \frac{\int_{\lambda_i}^{\lambda_f} \lambda f_{\lambda} S_{\lambda} d\lambda}{\int_{\lambda_i}^{\lambda_f} \lambda S_{\lambda} d\lambda} \quad (3)$$

where f_{λ} is the flux at a given wavelength λ and S_{λ} is the filter response at a given wavelength. The integration limits are the minimum and maximum wavelength of the bandpass.

4.2 Observed Fluxes

The observed, extinction corrected, magnitudes were transformed to fluxes using the standard formulas. For SDSS bandpasses (Fukugita et al. 1996),

$$m_{AB} = -2.5 \log f_{\nu} - 48.6 \quad (4)$$

The FUV and NUV fluxes are determined by means of the conversion,

$$m_{FUV} = -2.5 \log \frac{Flux_{FUV}}{1.40 * 10^{-15}} + 18.82 \quad (5)$$

$$m_{NUV} = -2.5 \log \frac{Flux_{NUV}}{2.06 * 10^{-16}} + 20.08 \quad (6)$$

4.3 SED Fitting

In the fitting process we minimize the following chi-square function:

$$\chi^2 = \sum_i \frac{(\alpha^2 f_{wd,i} + \beta^2 f_{bs,i} - F_i)^2}{\sigma_{F,i}^2} \quad (7)$$

Where i sum over all bandpasses.

$f_{bs,i}$, $f_{wd,i}$, F_i are the flux of the BS model, flux of the WD model and flux of the observed star respectively. $\alpha = (R_{bs}/D)$ and $\beta = (R_{wd}/D)$ are scale factors depend on radii (R_{bs} and R_{wd}) of each component and the distance (D).

The radii of both components (R_{bs} , R_{wd}) and distance are necessary as scale factors for the individual fluxes when combining the atmosphere models of both components to a single SED. However, for WD models the mass and the surface gravity is known. So for each model in the grid we can calculate the radius, according to:

$$R_{WD} = \sqrt{\frac{GM_{WD}}{g_{WD}}} \quad (8)$$

For the BS, we first obtain absolute magnitude calibration for our sample. we used transformation equations given by Zhao and Newberg (2006), which were derived from the SDSS stars with known UBVRI photometry, including a sample of BSS stars.

$$V = g - 0.561(g - r) - 0.004 \quad (9)$$

$$(B - V) = 0.916(g - r) + 0.187 \quad (10)$$

These transformations are valid within the range $-0.5 < g - r < 1.0$, (Beers et al. 2012) which is consistent with the color range we adopted here.

Using the V magnitude we obtained from equation 9, we can now calculate the absolute magnitude in V band (M_V) using the relation given by Kinman et al. (1994):

$$M_V = 1.32 + 4.05(B - V) - 0.45 \left[\frac{Fe}{H} \right] \quad (11)$$

This relation was constructed by studying the BSs in globular clusters with different metallicities covering a wide range of colors and absolute magnitudes.

The luminosity of the star can be found by use of M_V and bolometric correction in equation 12.

$$\left(\frac{L}{L_o} \right) = 10^{-0.4[M_V - V_o - 31.752 + (BC_V - BC_{V,o})]} \quad (12)$$

where we adopt the bolometric corrections given by Torres (2010).

Then, the radius of the BS can be estimated by use of the relation,

$$\left(\frac{R}{R_o} \right) = \left(\frac{T_o}{T_{eff}} \right)^2 \left(\frac{L}{L_o} \right)^{0.5} \quad (13)$$

To select the best fit white dwarf model, the χ^2 value of each fit is calculated by use of equation 7. The optimal SED fits for four stars are shown in the top panel of Figure 2. The presence of a hot white dwarf companion in a BS binary causes the excess FUV emission of the system. This is clear in Figure 2. The expected emission from BSs without WD companions is much fainter than the observed flux at FUV. Adding WD companions of increasing temperature results in bright, blue emission as evidence by the best fitting composite model (Black line in Figure 2: Top panel).

4.4 WD Parameters

The distributions of mass, age and effective temperatures of the white dwarfs determined from our SED fitting routine are shown in the bottom panel of Figure 2. The most striking features of the distributions are: Vast majority of white dwarfs are very young (few million years old) and with temperatures range between 20000 - 40000 K (See bottom panel of figure 2). This is consistent with our initial selection criteria of BS, as recently formed BS are expected to have much

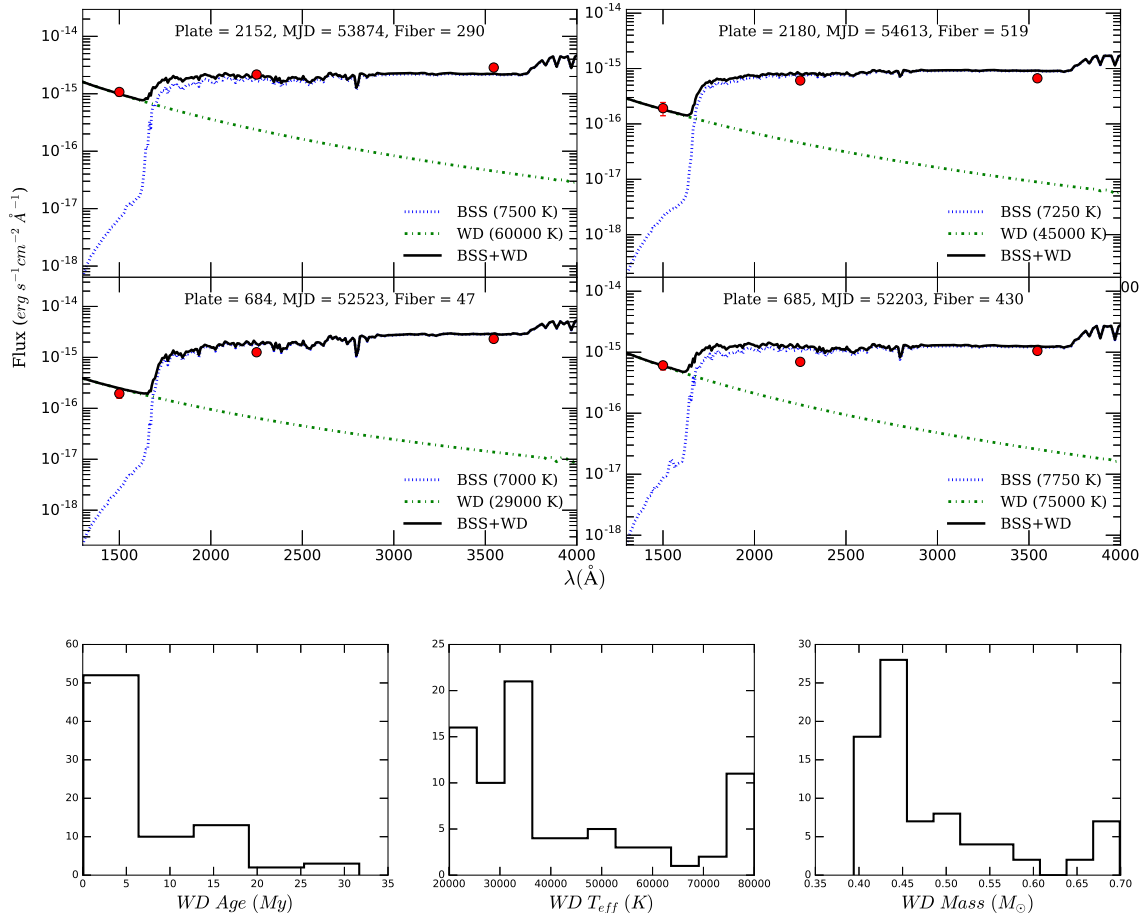


Figure 2. Top panel: Examples of BS+WD fitting. Red circles are the observed FUV,NUV and u band fluxes. Blue and green dashed lines represent the synthetic spectra of BS and WD respectively. Black solid line is the composite (BS+WD) best fit spectrum to the observed fluxes. Bottom panel: White Dwarf parameter distributions obtained from SED fitting.

larger UV excess. One interesting feature of the mass distribution is the peak at white dwarf mass $0.43 M_{\odot}$. White dwarf stars with masses below $0.47 M_{\odot}$ are thought to be He-core white dwarfs. (Core helium ignition starts when the core mass is roughly $0.47 M_{\odot}$) At the stage when mass transfer occurs, the expanding red giant core has not yet fully grown, therefore the resultant white dwarf will have a lower mass. If these WDs were single stars, they would have main sequence life times greater than age of the Universe. Therefore, these systems must be products of case B mass transfer, the only possible solution for producing such low mass white dwarfs.

On the other hand white dwarfs with masses $> 0.5 M_{\odot}$ are consistent with predictions from the case C, i.e., mass transfer from an asymptotic giant to a main sequence star which produces a carbon - oxygen white dwarf companion with mass of $\sim 0.5 M_{\odot}$ to $0.6 M_{\odot}$ dictated by the core mass of the asymptotic giant donor at the end of the mass transfer phase (Hurley et al. 2002). The WD Mass distribution in the Galactic field peaks at about $0.59 M_{\odot}$ and exhibits a significant low-mass tail of white dwarfs with masses lower than $0.45 M_{\odot}$ which peaks at $0.40 M_{\odot}$. These white dwarfs are predominantly found in close binary systems,

mostly with another white dwarf or a neutron star companion (Momány et al. 2004). Interestingly, the low mass end of this distribution is consistent with our results as well.

4.5 Mass Transfer efficiency

Mass transfer efficiency β , is defined as the mass fraction of the lost mass from the primary accreted by the secondary. This is an important parameter for binary evolution calculations where β is frequently treated with a constant value due to its large uncertainty. (De Greve and De Loore 1992; Chen and Han 2009). Lu et al. (2010) used Monte Carlo simulations to investigate the origin of BS population in M67. In their calculations they used the $\beta = 0.5$ and $\beta = 1.0$ (fully conservative mass transfer, i.e. no mass or angular momentum loss from the system) and found that the higher value could reproduce the data better. Our WD parameters obtained via the BS-WD fitting can be used to infer a lower limit for β in our current sample.

The amount of mass transferred from the now WD to BS, δM_t ,

$$\delta M_{trans} = M_i - M_{wd} \quad (14)$$

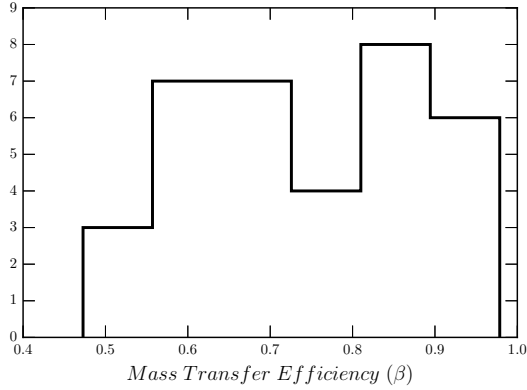


Figure 3. Histogram of the lower limits of the mass transfer efficiencies.

where M_i is the progenitor mass of the WD.

We interpolate theoretical relations which were constructed using BaSTI evolutionary models (Pietrinferni et al. 2006) so that we can calculate the progenitor mass at a given metallicity and age. We adopted the non-canonical BaSTI models with the mass loss efficiency of the Reimers law (Reimers 1977) set to $\eta = 0.2$. The initial He mass fraction ranges from 0.245 to 0.303, for the more metal-poor to the more metal-rich composition, respectively.

Jofré and Weiss (2011) estimated the ages of field halo stars using a sample of SDSS stars. They estimated a mean age 11 Gy, which we adopted in our calculations to determine the mass from interpolated BASTI models. The field stars of Jofré and Weiss (2011) have a mean metallicity of -1.7 dex. To be consistent with that work we limited our sample to the stars with $[Fe/H] < -1.35$. This reduces our sample to 35 stars.

To calculate the amount of mass transferred, the initial mass of the secondary star (Now the BS) is required. This initial mass value cannot be readily inferred, without first knowing the value of β . But we can estimate the lower limit of the transferred mass by considering the halo turnoff mass of $0.8 M_{\odot}$, Then the mass accreted on to the secondary (now BS) is given by,

$$\delta M_{acc} = M_{BS} - 0.8 \quad (15)$$

Ratio of equations 15 and 14 will give the lower limit of the mass transfer efficiency. The derived β values are shown as a histogram in Figure 3. All the stars have mass transfer efficiencies above $\beta \sim 0.5$. The value we obtained for the lower limit of β provides clues about the nature of these ancient, low-mass binary systems. The tendency for our systems to favor a more conservative mass transfer (larger β), should help to inform transfer models where donor initial mass less than $1.0 M_{\odot}$.

5 SUMMARY

We utilized UV-optical SED study of the BS binaries in the Galactic field. Using our fitting routine we identified WD companions of field BSs formed by mass transfer. We found

that these BSs have significant FUV excess by comparing the observed SED to a composite model with WD and BS components.

We found that our sample WDs range in age from a few million to a few tens of millions of years old, suggesting mass transfer in these binaries ended relatively recently. In addition we conclude that majority of the WD companions are helium WDs. Mass transfer from RGB stars in binary systems is the obvious way to produce such low mass stars.

Combining the WD stellar parameters with the evolutionary models we estimated the lower limit of the binary mass transfer efficiency in these stars to be, $\beta = 0.5$.

In order to determine the exact formation mechanisms for a particular population of BSs a detailed characterization of the BSs is needed. This requires determining the rotation velocities and binary orbital parameters. Since the formation channel for BS binaries can distinguish from the type of companion star expected, it is vital to identify the observational constraints of the companion. These binaries will be good test cases for binary mass transfer modeling efforts in the future.

ACKNOWLEDGEMENTS

The authors would like to thank our referee, George Preston, for his insightful comments and suggestions which improved the overall content and flow of this paper.

This work made use of the public data services provided by MAST and SDSS.

REFERENCES

- Beers et.al., The Case for the Dual Halo of the Milky Way. *ApJ*, 746:34, February 2012.
- Castelli and Kurucz, New Grids of ATLAS9 Model Atmospheres. *ArXiv Astrophysics e-prints*, May 2004.
- Chen and Han, Primordial binary evolution and blue stragglers. *MNRAS*, 395:1822–1836, June 2009. s
- De Greve and C. De Loore, Evolution of massive close binaries. *A&AS*, 96:653–663, December 1992.
- Deng et.al., The Blue Stragglers in M67 and Single-Population Synthesis. *ApJ*, 524:824–830, October 1999.
- Ferraro et al., Blue Straggler Stars: The Spectacular Population in M80. *ApJ*, 522:983–990, September 1999.
- Fontaine et.al, The Potential of White Dwarf Cosmochronology. *PASP*, 113:409–435, April 2001.
- Fukugita et.al., The Sloan Digital Sky Survey Photometric System. *AJ*, 111:1748, April 1996.
- Gosnell et.al., Detection of White Dwarf Companions to Blue Stragglers in the Open Cluster NGC 188: Direct Evidence for Recent Mass Transfer. *ApJ*, 783:L8 (5pp), March 2014.
- Gray and Corbally, The calibration of MK spectral classes using spectral synthesis. 1: The effective temperature calibration of dwarf stars *AJ*, 107-742, February 1994
- Hurley et.al., Evolution of binary stars and the effect of tides on binary populations. *MNRAS*, 329:897–928, February 2002.
- Jofré and A. Weiss. (2011), The age of the Milky Way halo stars from the Sloan Digital Sky Survey. *A&A*, 533:A59, September 2011.
- Kinman et al. The structure of the galactic halo outside the solar circle as traced by the blue horizontal branch stars. *AJ*, 108:1722–1772, November 1994.

- Kippenhahn and Weigert, Entwicklung in engen Doppelsternsystemen I. Massenaustausch vor und nach Beendigung des zentralen Wasserstoff-Brennens. *Z. Astrophys.*, 65:251, 1967.
- Lee et al., The SEGUE Stellar Parameter Pipeline. I. Description and Comparison of Individual Methods. *AJ*, 136:2022–2049, November 2008.
- Lu P. et al., Blue straggler formation via close binary mass transfer *MNRAS*, 409:1013–1021, December 2010.
- McCrea, Extended main-sequence of some stellar clusters. *MNRAS*, 128:147, 1964.
- Momány et al., The blue plume population in dwarf spheroidal galaxies. Genuine blue stragglers or young stellar population? *A&A*, 468:973–978, June 2007.
- Momány et al., Probing the Canis Major stellar over-density as due to the Galactic warp. *A&A*, 421:L29–L32, July 2004.
- Pietrinferni et al., A Large Stellar Evolution Database for Population Synthesis Studies. II. Stellar Models and Isochrones for an α -enhanced Metal Distribution. *ApJ*, 642:797–812, May 2006.
- Preston and Landolt, Pulsating Blue Metal-poor Stars. *AJ*, 118:3006–3015, December 1999.
- Preston and Sneden, What Are These Blue Metal-Poor Stars? *AJ*, 120:1014–1055, August 2000.
- Rebassa-Mansergas et al. Post-common envelope binaries from SDSS - XIV. The DR7 white dwarf-main-sequence binary catalogue. *MNRAS*, 419:806–816, January 2012.
- Rey et al., GALEX Ultraviolet Photometry of Globular Clusters in M31: Three-Year Results and a Catalog. *ApJS*, 173:643–658, December 2007.
- Ryan et al., Rapid Rotation of Ultra-Li-depleted Halo Stars and Their Association with Blue Stragglers. *ApJ*, 571:501–511, May 2002.
- Sandage A. R., The color-magnitude diagram for the globular cluster M3. 58:61–75, 1953.
- Mathieu and Geller, A binary star fraction of 76 per cent and unusual orbit parameters for the blue stragglers of NGC 188. *Nature*, 462:1032–1035, December 2009.
- Schlafly and Finkbeiner, Measuring Reddening with Sloan Digital Sky Survey Stellar Spectra and Recalibrating SFD. *ApJ*, 737:103, August 2011.
- Schlegel et al. Maps of Dust Infrared Emission for Use in Estimation of Reddening and Cosmic Microwave Background Radiation Foregrounds. *ApJ*, 500:525–553, June 1998.
- Sirko et al., Blue Horizontal-Branch Stars in the Sloan Digital Sky Survey. II. Kinematics of the Galactic Halo. *AJ*, 127:914–924, February 2004.
- Smith M. A. Interesting Features in the Combined GALEX and Sloan Color Diagrams of Solar like Galactic Populations. *AJ*, 147:159–1, June 2014.
- Tamás Budavári et al., Galex-sdss catalogs for statistical studies. *The Astrophysical Journal*, 694(2):1281, 2009.
- Torres, On the Use of Empirical Bolometric Corrections for Stars. *AJ*, 140:1158–1162, November 2010.
- Wheeler, Blue stragglers as long-lived stars. *ApJ*, 234:569–578, December 1979.
- Wood M.A., Theoretical White Dwarf Luminosity Functions: DA Models. volume 443 of *Lecture Notes in Physics, Berlin Springer Verlag*, page 41, 1995.
- Xue et al., The Milky Way's Circular Velocity Curve to 60 kpc and an Estimate of the Dark Matter Halo Mass from the Kinematics of 2400 SDSS Blue Horizontal-Branch Stars. *ApJ*, 684:1143–1158, September 2008.
- Yanny et al., Identification of A-colored Stars and Structure in the Halo of the Milky Way from Sloan Digital Sky Survey Commissioning Data. *ApJ*, 540:825–841, September 2000.
- Zhao and H. J. Newberg, Transformation from SDSS Photometric System to Johnson-Morgan-Cousins System in HK Survey. *ArXiv Astrophysics e-prints*, December 2006.

APPENDIX A:

Table A1. Stellar parameters and photometry of UV-excess BSs

SDSS ID	T_{eff}	$\log g$	$[Fe/H]$	FUV	NUV	u	g	r	i	z
915-52443-549	7423 ± 157	3.84 ± 0.49	-0.69 ± 0.2	19.0 ± 0.17	17.13 ± 0.04	15.76 ± 0.02	14.71 ± 0.01	14.68 ± 0.02	14.73 ± 0.01	14.82 ± 0.02
740-52263-440	7673 ± 129	4.32 ± 0.15	-1.98 ± 0.07	19.89 ± 0.24	19.35 ± 0.13	18.64 ± 0.02	17.84 ± 0.01	17.89 ± 0.01	17.94 ± 0.02	18.07 ± 0.03
684-52523-47	7004 ± 40	3.88 ± 0.23	-0.78 ± 0.05	20.93 ± 0.21	18.06 ± 0.03	16.41 ± 0.03	15.44 ± 0.02	15.3 ± 0.01	15.27 ± 0.02	15.34 ± 0.02
3131-54731-429	7936 ± 110	4.36 ± 0.03	-1.35 ± 0.1	20.08 ± 0.25	19.57 ± 0.07	18.55 ± 0.03	17.53 ± 0.02	17.56 ± 0.01	17.62 ± 0.01	17.59 ± 0.03
2951-54592-114	7615 ± 73	3.93 ± 0.44	-2.07 ± 0.16	19.42 ± 0.24	18.64 ± 0.1	17.55 ± 0.02	16.51 ± 0.02	16.49 ± 0.01	16.54 ± 0.01	16.57 ± 0.02
2849-54454-349	7083 ± 37	4.21 ± 0.29	-1.53 ± 0.02	19.46 ± 0.18	17.57 ± 0.05	16.22 ± 0.01	15.32 ± 0.02	15.2 ± 0.02	15.16 ± 0.01	15.22 ± 0.02
1894-53240-211	7441 ± 78	4.19 ± 0.21	-1.25 ± 0.08	21.18 ± 0.26	19.58 ± 0.04	18.48 ± 0.02	17.44 ± 0.02	17.33 ± 0.01	17.37 ± 0.01	17.43 ± 0.02
2299-53711-626	7742 ± 64	3.93 ± 0.18	-0.25 ± 0.04	21.67 ± 0.43	20.53 ± 0.19	18.71 ± 0.03	17.61 ± 0.01	17.61 ± 0.01	17.7 ± 0.02	17.81 ± 0.03
2299-53711-453	7460 ± 50	3.88 ± 0.21	-0.24 ± 0.08	21.01 ± 0.48	19.53 ± 0.16	17.69 ± 0.02	16.5 ± 0.01	16.45 ± 0.01	16.5 ± 0.01	16.58 ± 0.01
2848-54453-473	7032 ± 31	4.14 ± 0.25	-1.41 ± 0.04	19.47 ± 0.1	17.15 ± 0.02	15.9 ± 0.01	14.95 ± 0.02	14.82 ± 0.02	14.81 ± 0.02	14.88 ± 0.01
1254-52972-515	7672 ± 140	4.2 ± 0.11	-0.02 ± 0.05	18.66 ± 0.38	17.5 ± 0.12	15.96 ± 0.02	15.01 ± 0.01	15.07 ± 0.02	15.15 ± 0.01	15.33 ± 0.01
1252-52970-306	7791 ± 0	4.14 ± 0.23	-0.25 ± 0.03	16.95 ± 0.11	16.75 ± 0.06	16.28 ± 0.02	15.4 ± 0.02	15.41 ± 0.01	15.48 ± 0.01	15.61 ± 0.02
2335-53730-480	7468 ± 33	3.98 ± 0.31	-0.49 ± 0.14	19.14 ± 0.46	17.75 ± 0.15	16.04 ± 0.05	14.98 ± 0.02	14.9 ± 0.02	14.97 ± 0.02	15.02 ± 0.02
3241-54884-335	8029 ± 71	4.13 ± 0.2	-1.97 ± 0.25	19.3 ± 0.21	18.9 ± 0.13	18.16 ± 0.04	17.23 ± 0.02	17.32 ± 0.01	17.42 ± 0.01	17.54 ± 0.02
685-52203-430	7686 ± 112	3.93 ± 0.36	-1.03 ± 0.07	19.69 ± 0.17	18.7 ± 0.08	17.26 ± 0.01	16.11 ± 0.02	16.09 ± 0.02	16.12 ± 0.02	16.15 ± 0.02
3130-54740-107	7344 ± 69	4.15 ± 0.22	-1.89 ± 0.07	19.87 ± 0.19	19.32 ± 0.07	18.45 ± 0.02	17.45 ± 0.02	17.38 ± 0.01	17.35 ± 0.02	17.43 ± 0.02
2252-53565-281	7301 ± 44	4.19 ± 0.16	-0.27 ± 0.04	21.02 ± 0.39	19.05 ± 0.05	17.4 ± 0.01	16.32 ± 0.02	16.24 ± 0.01	16.26 ± 0.01	16.3 ± 0.01
1961-53299-168	7291 ± 45	4.05 ± 0.19	-0.76 ± 0.02	19.49 ± 0.17	18.25 ± 0.07	17.61 ± 0.02	16.61 ± 0.01	16.53 ± 0.02	16.54 ± 0.02	16.62 ± 0.02
1960-53289-343	7127 ± 33	4.23 ± 0.17	-0.54 ± 0.06	20.9 ± 0.4	18.45 ± 0.09	16.71 ± 0.02	15.68 ± 0.02	15.54 ± 0.01	15.54 ± 0.02	15.57 ± 0.02
3138-54740-521	7381 ± 31	4.03 ± 0.3	-1.11 ± 0.03	21.04 ± 0.45	19.95 ± 0.19	18.44 ± 0.03	17.4 ± 0.01	17.31 ± 0.01	17.35 ± 0.02	17.38 ± 0.02
3138-54740-401	7562 ± 177	4.31 ± 0.16	-2.59 ± 0.01	19.49 ± 0.21	19.08 ± 0.12	17.77 ± 0.03	16.76 ± 0.01	16.75 ± 0.01	16.73 ± 0.01	16.71 ± 0.02
1857-53182-27	7343 ± 129	4.31 ± 0.2	-0.88 ± 0.08	21.53 ± 0.34	20.45 ± 0.19	18.87 ± 0.03	17.9 ± 0.01	17.77 ± 0.01	17.79 ± 0.01	17.88 ± 0.03
366-52017-28	7320 ± 60	4.2 ± 0.23	-1.01 ± 0.08	21.16 ± 0.37	19.37 ± 0.12	17.88 ± 0.02	16.91 ± 0.02	16.86 ± 0.01	16.86 ± 0.02	16.92 ± 0.02
2797-54616-614	8005 ± 47	4.24 ± 0.19	-1.22 ± 0.32	20.87 ± 0.38	20.41 ± 0.26	18.74 ± 0.04	17.67 ± 0.01	17.71 ± 0.01	17.81 ± 0.02	17.92 ± 0.03
2551-54552-257	7368 ± 100	4.07 ± 0.06	-1.31 ± 0.06	21.51 ± 0.34	19.91 ± 0.12	18.75 ± 0.02	17.58 ± 0.02	17.51 ± 0.02	17.52 ± 0.02	17.52 ± 0.03
2247-53875-96	7290 ± 68	4.18 ± 0.29	-0.54 ± 0.04	20.57 ± 0.34	19.57 ± 0.14	18.18 ± 0.02	17.1 ± 0.02	17.05 ± 0.01	17.08 ± 0.01	17.15 ± 0.02
2180-54613-519	7368 ± 46	3.98 ± 0.31	-1.83 ± 0.01	20.94 ± 0.29	18.85 ± 0.06	17.75 ± 0.02	16.89 ± 0.02	16.87 ± 0.02	16.87 ± 0.02	16.92 ± 0.02
1659-53224-452	7530 ± 40	4.05 ± 0.19	-0.56 ± 0.09	19.56 ± 0.15	17.9 ± 0.05	16.46 ± 0.02	15.39 ± 0.01	15.38 ± 0.01	15.45 ± 0.02	15.55 ± 0.02
2550-54206-232	7097 ± 80	4.24 ± 0.14	-0.97 ± 0.05	21.17 ± 0.36	18.61 ± 0.07	17.16 ± 0.02	16.15 ± 0.01	16.04 ± 0.02	16.02 ± 0.02	16.04 ± 0.02
2189-54624-640	7307 ± 61	4.0 ± 0.67	-1.5 ± 0.0	21.51 ± 0.45	19.91 ± 0.11	18.71 ± 0.03	17.74 ± 0.02	17.73 ± 0.01	17.75 ± 0.01	17.84 ± 0.03
595-52023-92	7542 ± 81	4.11 ± 0.08	-1.72 ± 0.04	19.07 ± 0.18	17.99 ± 0.05	16.88 ± 0.02	15.89 ± 0.01	15.87 ± 0.01	15.92 ± 0.01	15.98 ± 0.02
1727-53859-288	7045 ± 39	3.84 ± 0.43	-0.53 ± 0.02	21.79 ± 0.43	20.25 ± 0.14	18.61 ± 0.02	17.52 ± 0.02	17.42 ± 0.02	17.42 ± 0.02	17.48 ± 0.02
2782-54592-113	7445 ± 103	3.88 ± 0.45	-1.61 ± 0.05	19.64 ± 0.21	19.26 ± 0.12	18.33 ± 0.02	17.23 ± 0.01	17.16 ± 0.01	17.12 ± 0.01	17.11 ± 0.02
3308-54919-447	7368 ± 82	3.92 ± 0.4	-1.41 ± 0.09	20.9 ± 0.37	19.81 ± 0.14	18.8 ± 0.03	17.95 ± 0.02	17.91 ± 0.01	17.96 ± 0.02	18.04 ± 0.03
2781-54266-417	7768 ± 145	4.37 ± 0.16	-1.34 ± 0.03	20.35 ± 0.26	19.28 ± 0.11	18.16 ± 0.02	17.23 ± 0.02	17.31 ± 0.01	17.34 ± 0.01	17.41 ± 0.02
2156-54525-520	7483 ± 58	3.89 ± 0.42	-0.98 ± 0.02	21.75 ± 0.42	20.26 ± 0.14	18.71 ± 0.02	17.7 ± 0.01	17.68 ± 0.02	17.74 ± 0.01	17.83 ± 0.02
3297-54941-411	7411 ± 56	3.98 ± 0.45	-1.14 ± 0.17	19.99 ± 0.28	18.52 ± 0.08	17.34 ± 0.02	16.33 ± 0.02	16.27 ± 0.02	16.3 ± 0.02	16.32 ± 0.02
2152-53874-290	7557 ± 40	4.14 ± 0.23	-1.02 ± 0.09	19.07 ± 0.16	17.47 ± 0.05	16.17 ± 0.01	15.11 ± 0.02	15.11 ± 0.01	15.17 ± 0.01	15.26 ± 0.02
3406-54970-104	7191 ± 81	4.32 ± 0.02	-1.98 ± 0.02	21.27 ± 0.32	19.92 ± 0.11	18.77 ± 0.02	17.87 ± 0.02	17.79 ± 0.02	17.77 ± 0.03	17.83 ± 0.02
3406-54970-518	7335 ± 50	4.25 ± 0.18	-1.79 ± 0.04	21.91 ± 0.44	19.89 ± 0.11	18.8 ± 0.02	17.9 ± 0.02	17.8 ± 0.01	17.82 ± 0.01	17.86 ± 0.03
3387-54951-106	7979 ± 116	4.21 ± 0.38	-1.84 ± 0.21	20.53 ± 0.4	20.07 ± 0.2	18.75 ± 0.02	17.73 ± 0.02	17.73 ± 0.02	17.87 ± 0.02	17.99 ± 0.02
3384-54948-315	7403 ± 67	3.89 ± 0.33	-1.92 ± 0.07	21.29 ± 0.28	19.45 ± 0.07	18.29 ± 0.02	17.3 ± 0.02	17.24 ± 0.02	17.25 ± 0.02	17.32 ± 0.02
1348-53084-179	7652 ± 15	4.19 ± 0.21	-2.24 ± 0.0	19.6 ± 0.18	18.53 ± 0.06	17.59 ± 0.02	16.59 ± 0.01	16.59 ± 0.02	16.67 ± 0.02	16.69 ± 0.02
2124-53770-535	7005 ± 44	4.08 ± 0.04	-1.45 ± 0.05	21.25 ± 0.45	18.57 ± 0.09	17.13 ± 0.02	16.25 ± 0.01	16.12 ± 0.01	16.12 ± 0.01	16.15 ± 0.01
2336-53712-115	7469 ± 22	4.07 ± 0.23	-0.6 ± 0.07	21.01 ± 0.4	19.96 ± 0.19	18.5 ± 0.02	17.46 ± 0.02	17.4 ± 0.01	17.45 ± 0.01	17.52 ± 0.02
424-51893-60	7176 ± 23	3.93 ± 0.11	-0.61 ± 0.09	21.31 ± 0.46	18.84 ± 0.09	17.09 ± 0.02	16.04 ± 0.02	15.94 ± 0.02	15.95 ± 0.01	16.0 ± 0.02
2445-54573-173	7317 ± 87	4.25 ± 0.34	-1.37 ± 0.46	21.78 ± 0.34	19.85 ± 0.1	18.72 ± 0.02	17.66 ± 0.02	17.57 ± 0.02	17.65 ± 0.02	17.69 ± 0.02
1282-52759-79	7541 ± 52	3.83 ± 0.35	-1.8 ± 0.13	21.1 ± 0.37	19.53 ± 0.11	18.32 ± 0.02	17.22 ± 0.03	17.23 ± 0.01	17.29 ± 0.01	17.36 ± 0.02
3377-54950-189	7349 ± 31	4.13 ± 0.35	-1.38 ± 0.09	19.95 ± 0.21	18.83 ± 0.07	17.75 ± 0.02	16.84 ± 0.01	16.78 ± 0.01	16.81 ± 0.02	16.84 ± 0.02
2899-54568-252	7164 ± 29	4.01 ± 0.12	-0.22 ± 0.05	20.04 ± 0.23	17.51 ± 0.04	15.63 ± 0.03	14.57 ± 0.02	14.46 ± 0.02	14.47 ± 0.01	14.56 ± 0.02
1456-53115-620	7072 ± 59	3.9 ± 0.27	-0.84 ± 0.04	21.53 ± 0.48	18.97 ± 0.05	17.32 ± 0.02	16.22 ± 0.02	16.14 ± 0.02	16.18 ± 0.02	16.24 ± 0.02
2661-54505-400	7402 ± 59	4.13 ± 0.12	-0.7 ± 0.08	20.64 ± 0.27	18.93 ± 0.05	17.65 ± 0.02	16.61 ± 0.02	16.59 ± 0.01	16.62 ± 0.01	16.71 ± 0.01
335-52000-452	7758 ± 159	4.1 ± 0.16	-2.03 ± 0.06	19.58 ± 0.19	19.11 ± 0.1	18.49 ± 0.02	17.54 ± 0.02	17.61 ± 0.01	17.66 ± 0.01	17.7 ± 0.02
2647-54495-235	7096 ± 51	3.9 ± 0.12	-1.47 ± 0.02	21.61 ± 0.42	19.04 ± 0.09	17.62 ± 0.02	16.66 ± 0.02	16.56 ± 0.02	16.55 ± 0.02	16.59 ± 0.02
3253-54941-210	7296 ± 41	3.96 ± 0.27	-1.74 ± 0.04	21.47 ± 0.47	19.29 ± 0.07	17.99 ± 0.02	17.06 ± 0.02	17.0 ± 0.02	17.03 ± 0.02	17.08 ± 0.02
334-51993-267	7270 ± 74	3.94 ± 0.28	-1.38 ± 0.01	21.78 ± 0.41	20.32 ± 0.13	18.76 ± 0.02	17.7 ± 0.02	17.63 ± 0.02	17.66 ± 0.01	17.71 ± 0.02
3214-54866-426	7159 ± 49	3.85 ± 0.3	-1.68 ± 0.04	21.69 ± 0.48	19.99 ± 0.16	18.55 ± 0.04	17.6 ± 0.02	17.57 ± 0.02	17.55 ± 0.02	17.61 ± 0.02
2892-54552-128	7256 ± 80	3.84 ± 0.37	-1.99 ± 0.13	22.22 ± 0.3	19.94 ± 0.08	18.67 ± 0.02	17.82 ± 0.02	17.71 ± 0.01	17.71 ± 0.01	17.77 ± 0.02
3285-54948-131	7509 ± 116	3.94 ± 0.2	-1.66 ± 0.02	18.48 ± 0.1	17.79 ± 0.05	16.93 ± 0.03	15.98 ± 0.03	16.03 ± 0.03	16.06 ± 0.02	16.14 ± 0.03
2512-53877-326	7061 ± 48	3.86 ± 0.16	-2.04 ± 0.09	21.44 ± 0.38	18.85 ± 0.04	17.48 ± 0.02	16.5 ± 0.01	16.41 ± 0.02	16.44 ± 0.01	16.46 ± 0.02
3170-54859-111	7520 ± 98	4.23 ± 0.31	-2.39 ± 0.05	20.12 ± 0.14	18.93 ± 0.04	17.87 ± 0.02	16.86 ± 0.01	16.82 ± 0.01	16.84 ± 0.02	16.89 ± 0.02
878-52353-617	7240 ± 51	4.14 ± 0.31	-1.81 ± 0.16	20.61 ± 0.3	18.79 ± 0.07	17.41 ± 0.02	16.44 ± 0.02	16.33 ± 0.02	16.36 ± 0.03	16.38 ± 0.02
3193-54830-593	7838 ± 78	4.19 ± 0.22	-1.14 ± 0.02	20.44 ± 0.22	19.71 ± 0.11	18.66 ± 0.03	17.55 ± 0.02	17.62 ± 0.01	17.66 ± 0.02	17.75 ± 0.03
267-51608-422	7336 ± 59	3.98 ± 0.32	-1.55 ± 0.06	21.55 ± 0.36	19.96 ± 0.1	18.5 ± 0.02	17.5 ± 0.02	17.44 ± 0.02	17.49 ± 0.02	17.56 ± 0.03
1739-53050-128	7533 ± 73	3.98 ± 0.16	-2.23 ± 0.05	20.89 ± 0.37	19.31 ± 0.08	18.01 ± 0.02	16.98 ± 0.02	16.81 ± 0.01	16.87 ± 0.02	17.13 ± 0.02
1934-53357-4	7408 ± 39	4.03 ± 0.09	-1.43 ± 0.15	21.64 ± 0.28	20.35 ± 0.12	19.02 ± 0.03	17.97 ± 0.03	17.95 ± 0.02	17.98 ± 0.02	18.02 ± 0.04
1590-52974-388	7126 ± 23	3.95 ± 0.05	-0.24 ± 0.02	21.86 ± 0.46	19.31 ± 0.1	17.71 ± 0.02	16.58 ± 0.01	16.49 ± 0.02	16.51 ± 0.02	16.57 ± 0.02
3195-54832-552	7059 ± 34	4.07 ± 0.14	-0.42 ± 0.03	20.81 ± 0.39	18.9 ± 0.1	17.32 ± 0.02	16.3 ± 0.02	16.22 ± 0.02	16.2 ± 0.01	16.26 ± 0.01
3230-54860-409	7081 ± 54	4.34 ± 0.14	-0.42 ± 0.							